Equatorial ligand effects on the diradical character dependence of the second hyperpolarizabilities of open-shell singlet transition-metal dinuclear complexes

ARTICLE *in* CHEMICAL PHYSICS LETTERS · MAY 2013

Impact Factor: 1.9 · DOI: 10.1016/j.cplett.2013.03.030

4 AUTHORS, INCLUDING:

Benoît Champagne
University of Namur
401 PUBLICATIONS **8,719** CITATIONS
SEE PROFILE

Masayoshi Nakano
Osaka University
337 PUBLICATIONS **4,769** CITATIONS
SEE PROFILE

Chemical Physics Letters 570 (2013) 75–79

Contents lists available at SciVerse ScienceDirect

Chemical Physics Letters

journal homepage: www.elsevier.com/locate/cplett

Equatorial ligand effects on the diradical character dependence of the second hyperpolarizabilities of open-shell singlet transition-metal dinuclear complexes

Yudai Inoue [a], Taishi Yamada [a], Benoît Champagne [b], Masayoshi Nakano [a,*]

[a] Department of Materials Engineering Science, Graduate School of Engineering Science, Osaka University, Toyonaka, Osaka 560-8531, Japan
[b] Laboratoire de Chimie Théorique, University of Namur, rue de Bruxelles, 61, B-5000 Namur, Belgium

ARTICLE INFO

Article history:
Received 14 February 2013
In final form 11 March 2013
Available online 28 March 2013

ABSTRACT

We investigate the equatorial ligand effects on the diradical character (y) dependence of the longitudinal second hyperpolarizability (γ) of the $Re(IV)_2F_8$ transition-metal dinuclear complex with different bond lengths using the spin-unrestricted coupled-cluster method. It is found that the equatorial ligands do not affect the intrinsic y–γ relationship nor the dσ-electron dominant contribution to the maximum γ (γ_{max}) observed in the bare dinuclear analogs but γ_{max} of $Re(IV)_2F_8$ is about one order of magnitude larger than that of $Re(IV)_2$.

1. Introduction

In previous studies [1–4], we have theoretically proposed open-shell singlet molecules as a novel class of nonlinear optical (NLO) systems and have revealed that singlet diradical systems with intermediate diradical characters exhibit larger second hyperpolarizabilities γ (the third-order NLO properties at the molecular scale) than pure diradical and closed-shell systems of similar size. The mechanism of this structure–property relationship has been unraveled by the valence configuration interaction (VCI) method based on a two-site diradical model [2,3], and has been exemplified by ab initio molecular orbital (MO) and density functional theory (DFT) studies on several model and real molecular systems [5–10]. These theoretical predictions have also been experimentally confirmed by two-photon absorption [11–13] and third-harmonic generation measurements [14].

As examples of open-shell singlet NLO compounds, we have investigated singlet transition-metal complexes with metal–metal multiple bonds [15–17] having multiple diradical characters, which originate from their weak d–d interactions. It has been found that the γ values of the singlet dichromium(II) (Cr(II)–Cr(II)) and dimolybdenum(II) (Mo(II)–Mo(II)) model systems with different metal–metal bond lengths, which vary the diradical characters of the dσ, dπ, and dδ orbitals (y(dσ), y(dπ), and y(dδ), respectively), are dominated by the dσ electrons, and that the γ values take maximum values in the intermediate y(dσ) region [8]. These features are predicted to be caused by the size of the valence d atomic orbital, and this prediction has been verified by examining γ of different metal–metal bonded systems [9]. These results provide a new guideline for an effective molecular design of highly efficient third-order NLO systems based on metal–metal bonded systems.

On the other hand, most transition-metal compounds exist as complexes including ligands, and the charge transfer between metal (M) and ligand (L) has been predicted to impact to the NLO responses [18]. Similarly, the open-shell characters of metal–metal bonds in those complexes are speculated to be significantly influenced by the metal–ligand interaction. It is therefore important to clarify the effects of the ligands on the diradical characters and the hyperpolarizabilities γ of metal–metal bonded systems. In this Letter, we examine the effect of equatorial ligands, involved in M_2L_8 complexes that consist of two square-planar or pyramidal (ML_4) units, on y and γ by comparing the results of $Re(IV)_2F_8$ with those of the corresponding bare dinuclear system, $Re(IV)_2$, which possesses a formally triple metal–metal bond composed of one dσ and two equivalent dπ bonds. $Re(IV)_2$ complexes belong to the real transition-metal complexes [15] and are expected to be prototypical for a wide range of diradical characters, that could be achieved by varying the metal–metal bond length as observed in other bare homodinuclear systems [9]. The present results will contribute to clarifying the origin of the NLO properties in real metal–metal multiply bonded complexes, as well as to assessing the applicability of our open-shell character based design guidelines for achieving remarkable NLO responses to transition metal complexes.

2. Model systems and calculation methods

We investigate $Re(IV)_2$ and $Re(IV)_2F_8$ as model systems. The $Re(IV)_2F_8$ model complex possesses an eclipsed M_2L_8 conformation

* Corresponding author. Fax: +81 6 6850 6268.
E-mail address: mnaka@cheng.es.osaka-u.ac.jp (M. Nakano).

0009-2614/$ - see front matter © 2013 Elsevier B.V. All rights reserved.
http://dx.doi.org/10.1016/j.cplett.2013.03.030

of symmetry D_{4h}, which is one of the major and simplest geometries observed in transition-metal complexes with metal–metal multiple bonds (see Figure 1). The Re–Re bond lengths observed in real $Re(IV)_2$ compounds range from 2.21 to 2.41 Å [15], for which the compounds are predicted to have almost closed-shell character ($y \sim 0$). In order to reveal the bond length dependences of the diradical characters as well as of the longitudinal γ values [along the bond (z) axis], Re–Re bond lengths (R) were varied from 2.6 to 4.0 Å, which leads to a wide range of diradical character ($0 < y < 1$). In this regard, we keep the other geometrical parameters to those of the equilibrium structure of $Re(IV)_2F_8$ optimized at the RB3LYP level of approximation under the constraint of D_{4h} symmetry. Such model is sufficient for the present study, which focuses on the clarification of the primary effects of the equatorial ligands on the diradical character and γ values.The diradical character (y_i) is defined as the occupation number ($n_{\mathrm{LUNO}+i}$) of the lowest unoccupied natural orbital (LUNO) + i (i = 0, 1,...) [19]. The diradical character can also be estimated using spin-unrestricted single determinant schemes like the spin-unrestricted Hartree–Fock (UHF) method. To avoid the spin contamination effects, the diradical characters based on UHF calculations are obtained using a perfect-pairing type spin-projection scheme [20],

$$y_i = 1 - \frac{2T_i}{1+T_i^2}, \quad \text{where} \quad T_i = \frac{n_{\mathrm{HONO}-i} - n_{\mathrm{LUNO}+i}}{2} \tag{1}$$

Here, y_i is referred to as the diradical character at the spin-projected UHF (PUHF) level of approximation. T_i (the orbital overlap between the corresponding orbital pairs) is expressed by the difference between $n_{\mathrm{HONO}-i}$ and $n_{\mathrm{LUNO}+i}$, which represent the occupation numbers of the HONO(=the highest occupied NOs)–i and LUNO + i, respectively. The PUHF y_i value ranges from 0 to 1, which represent closed-shell and pure diradical states, respectively. It has been shown to well reproduce the diradical character calculated by other methods such the ab initio configuration interaction (CI) method [21]. In the present study, the diradical character of the dX orbital (y(dX), where $X = \sigma, \pi$) is calculated by using Eq. (1) from the occupation number of the dX bonding and anti-bonding NO pairs [8,9]. In order to clarify the origin of the metal–metal bond-length (R) dependences of y(dX), we employ an analytical expression of y (Eq. (2)), which is derived from the expression obtained by the VCI two-site diradical model [2].

$$y(\mathrm{d}X) = 1 - \frac{1}{\sqrt{1+\left(\frac{K_{\mathrm{d}X}}{\varepsilon_{\mathrm{d}X}}\right)^2}}, \tag{2}$$

where $K_{\mathrm{d}X}$ ($\geqslant 0$) and $\varepsilon_{\mathrm{d}X}$ represent the exchange integral and the difference of diagonal Fock elements (orbital energy gap) between the symmetry-adapted bonding (g) and anti-bonding (u) MOs, related to the diradical character y(dX), respectively (see Supplementary data). Generally, the exchange integral is large when the g and u orbitals distribute over the same space, and particularly when these are localized. As seen from Eq. (2), the decrease in $K_{\mathrm{d}X}$ and/or the increase in $\varepsilon_{\mathrm{d}X}$ lead to the decrease in y(dX). The $K_{\mathrm{d}X}$ and $\varepsilon_{\mathrm{d}X}$ values associated with the dσ and dπ orbitals in $Re(IV)_2$ and $Re(IV)_2F_8$ at R = 2.6–4.0 Å, were evaluated from the excitation energies calculated at the CASCI(2,2) level using spin-unrestricted NOs (UNOs) (see Supplementary data). In addition, we analyze the results based on the spatial distributions of dσ and dπ UNOs. We observe that the R-dependent variations in y(dX) values ($X = \sigma, \pi$) obtained by using Eq. (2) and the UNOCASCI(2,2) solutions are in good agreement with those at the PUHF and UCCSD level of approximations (see Supplementary data). The UNOCASCI(2,2) calculations were performed using the GAMESS program package [22].

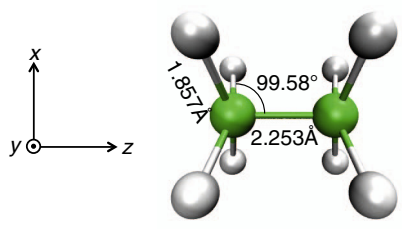

Figure 1. Structure of $Re(IV)_2F_8$, where green and white balls represent Re and F atoms, respectively. The metal–metal bond length R (Å) is varied from 2.6 to 4.0 Å with fixed metal–ligand bond lengths (1.857 Å) and bond angles (99.58°). Coordinate axes are also shown. (For interpretation of the references to color in this figure legend, the reader is referred to the web version of this book.)

The bond-axis component γ_{zzzz}(simply referred to as γ hereafter) is calculated using the finite-field (FF) approach [23], which consists in the forth-order differentiation of the total energy with respect to the applied external electric field. The perturbation series expansion convention (called B convention) is chosen for defining γ, and the following numerical differentiation formula is employed [24]:

$$\gamma = \frac{1}{36(F)^4}\{E(3F) - 12E(2F) + 39E(F) - 56E(0) + 39E(-F) - 12E(-2F) + E(-3F)\} \tag{3}$$

Here, $E(F)$ indicates the total energy in the presence of the static electric field F in the z-direction. We used F values ranging from 0.0010 to 0.0060 a.u. to obtain numerically stable γ values. Moreover, a tight convergence threshold of 10^{-10} a.u. on the energy is adopted to obtain numerically stable γ values. The γ values were calculated using the spin-unrestricted coupled cluster singles and doubles (UCCSD) as well as including the perturbative triples (UCCSD(T)). For a detailed analysis of γ, the dσ and dπ electron contributions to γ [γ(dX), where $X = \sigma, \pi$] were calculated along with the γ(dX) density by adopting the partitioning scheme of γ[19], where a given γ(dX) contribution is expressed as

$$\gamma(\mathrm{d}X) = -\frac{1}{3!}\int r\mathrm{d}^{\mathrm{d}X(3)}(\mathbf{r})d\mathbf{r}, \tag{4}$$

where $\mathrm{d}^{\mathrm{d}X(3)}(\mathbf{r})$ is obtained from the third-order derivatives of the electron densities of the bonding (dX) and anti-bonding (dX^*) NO pair with respect to the electric field in the z-direction:

$$\mathrm{d}^{\mathrm{d}X(3)}(\mathbf{r}) = \frac{\partial}{\partial F^3}[n_{\mathrm{d}X}\varphi^*_{\mathrm{d}X}(\mathbf{r})\varphi_{\mathrm{d}X}(\mathbf{r}) + n_{\mathrm{d}X^*}\varphi^*_{\mathrm{d}X^*}(\mathbf{r})\varphi_{\mathrm{d}X^*}(\mathbf{r})]. \tag{5}$$

Here, $\varphi_{\mathrm{d}X}(\mathbf{r})$ and $n_{\mathrm{d}X}$ represent the dX NO and its occupation number, respectively. The γ(dX) values were evaluated at the UCCSD level.

For the different calculations, we employed the effective core potential (ECP) of the Stuttgart group with corresponding valence basis set (SDD) for Re atoms [25], and 6-31G* basis sets for F atoms. The SDD basis set was supplemented with an additional f polarization function (ζ_f = 0.869) (referred to as 'SDD(f)' in this Letter) [26]. As previously found for closed-shell [27] and open-shell singlet systems [28,29], extended basis sets (with diffuse functions) are indispensable for obtaining quantitative γ values. In this point, the SDD basis set already includes one set of diffuse s, two sets of diffuse p, and one set of diffuse d functions, which should be sufficient for describing γ. In addition, owing to the anionic character of the ligands, extended basis sets with diffuse functions are also necessary to describe the ligands and to provide quantitative γ values of transition metal complexes [30–33]. Although the use of such extended basis sets on the ligands was not possible in this study due to the huge computational demands at the UCCSD level of theory, the primary ligand effects on the diradical character and on the γ values are correctly accounted for with the present

method. All the calculations were performed by GAUSSIAN 09 program package [34].

3. Results and discussion

3.1. Equatorial ligand effect on the diradical character

Figure 2 shows the bond length (R) dependence of the diradical characters for $Re(IV)_2$ and $Re(IV)_2F_8$. In both systems, the diradical characters $y(dX)$ ($X = \sigma, \pi$) increase as a function of R with keeping the $y(d\pi) > y(d\sigma)$ ordering for any R, which reflects the difference between the $d\pi-d\pi$ and $d\sigma-d\sigma$ overlaps. Also, at each R, the $y(dX)$ of $Re(IV)_2F_8$ is smaller than that of $Re(IV)_2$. Using Eq. (2), we investigate the variations in ε_{dX} and K_{dx} ($X = \sigma, \pi$) for $Re(IV)_2$ and $Re(IV)_2F_8$ as a function of R (see Figure 3). It is found that, when R increases, for both systems ε_{dX} decreases due to the decrease in d–d overlap, while K_{dx} increases due to the same reason, i.e., the bonding and anti-bonding dX orbitals become localized around the constituent metal atoms. In case of $d\sigma$ orbitals (Figure 3a), for any R, (i) the $K_{d\sigma}$ value of $Re(IV)_2F_8$ is smaller than that of $Re(IV)_2$, and (ii) the $\varepsilon_{d\sigma}$ value of $Re(IV)_2F_8$ is larger than that of $Re(IV)_2$. This explains why, using Eq. (2), $y(dX)$ decreases from $Re(IV)_2$ to $Re(IV)_2F_8$. The ligand effects on $\varepsilon_{d\sigma}$ and $K_{d\sigma}$ can be clarified by considering the bonding/anti-bonding orbital distributions in Figure 4. At $R = 2.6$ Å the $d\sigma$ bonding/anti-bonding characters of $Re(IV)_2F_8$ are stronger, i.e., the $d\sigma$ distributions in the inner and outer regions are more enhanced in the bonding and anti-bonding orbitals, respectively, than in $Re(IV)_2$ due to the repulsion between the $d\sigma$ electrons and the anionic equatorial ligands. This leads to the increase in $\varepsilon_{d\sigma}$ of $Re(IV)_2F_8$ as compared to $Re(IV)_2$ (see

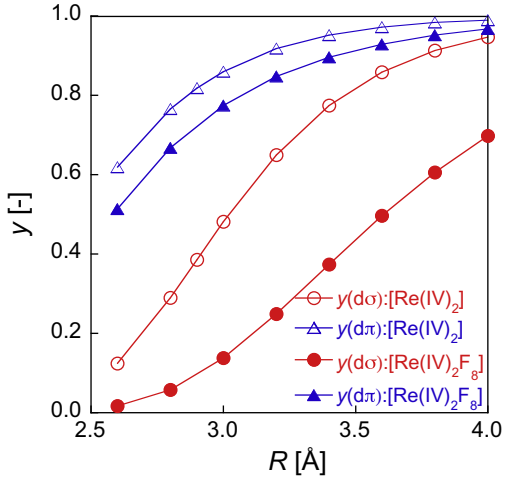

Figure 2. Variations of the diradical characters of dX orbitals ($y(dX)$, $X = \sigma$ and π) as a function of the metal–metal bond length (R) in $Re(IV)_2$ and $Re(IV)_2F_8$ obtained using the PUHF method.

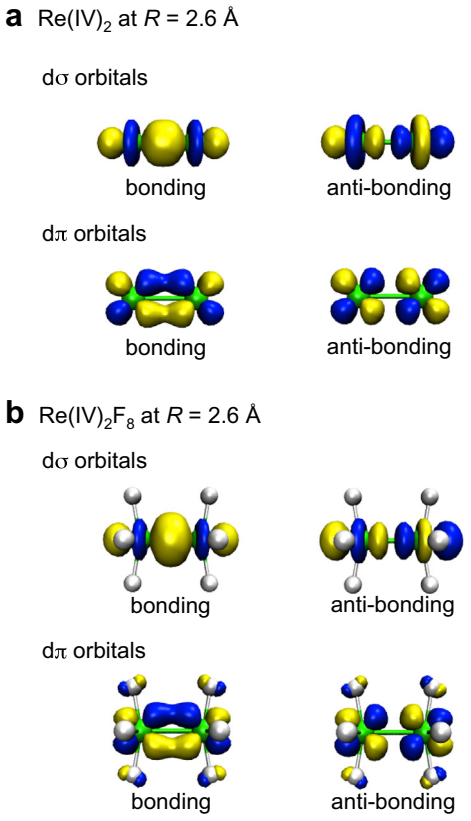

Figure 4. $d\sigma$ and $d\pi$ bonding/anti-bonding natural orbitals in $Re(IV)_2$ and $Re(IV)_2F_8$ with $R = 2.6$ Å obtained from the UHF solutions.

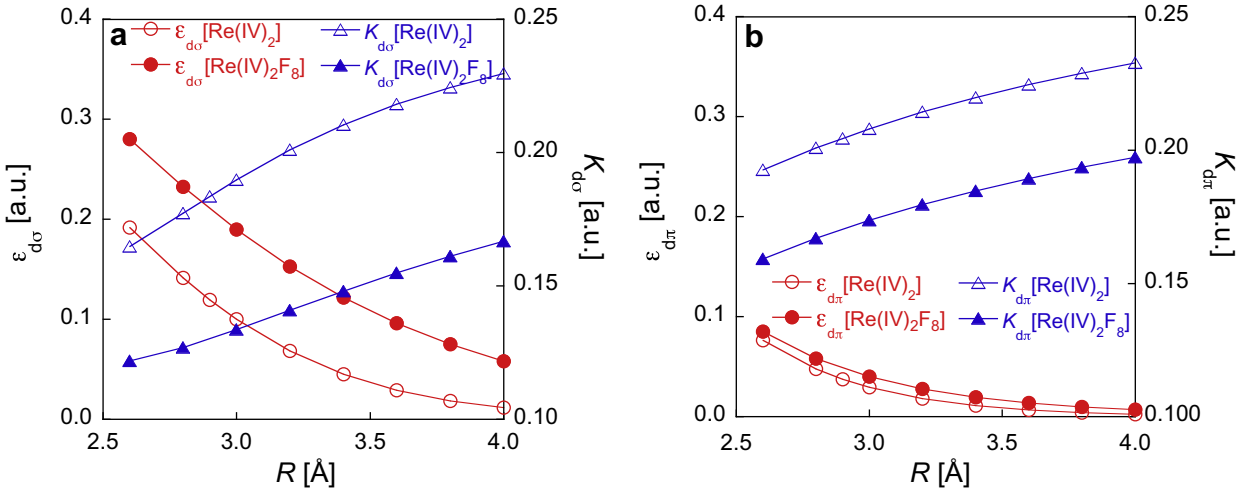

Figure 3. Metal–metal bond length (R) dependences of the orbital energy gap ε_{dX} and of the exchange integral K_{dx} for $X = \sigma$ (a) and π (b) in $Re(IV)_2$ and $Re(IV)_2F_8$ calculated using the UNOCASCI(2,2) method.

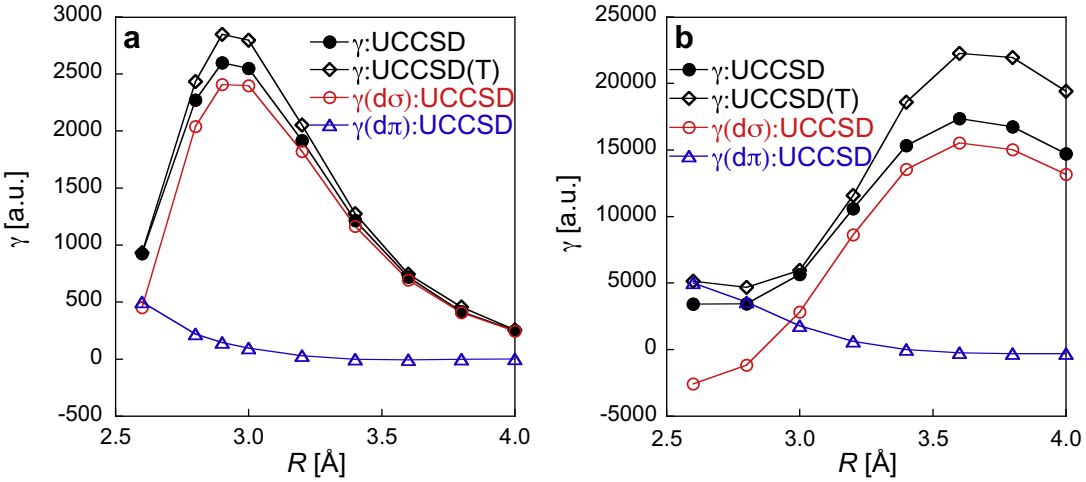

Figure 5. Metal–metal bond length (R) dependences of γ calculated using the UCCSD and UCCSD(T) methods as well as their dX contributions [γ(dX), $X = \sigma, \pi$] in $Re(IV)_2$ (a) and $Re(IV)_2F_8$ (b) calculated using the UCCSD method.

Figure 3a). This difference of bonding/anti-bonding dσ character causes also the decrease in $K_{d\sigma}$ of $Re(IV)_2F_8$ as compared to $Re(IV)_2$ because of the relative decrease in the overlap between the bonding and anti-bonding dσ orbitals in $Re(IV)_2F_8$.

In addition, (i) $K_{d\pi}$ of $Re(IV)_2$ is similar to (or slightly larger at small R than) $K_{d\sigma}$ and $\varepsilon_{d\pi}$ is much smaller than $\varepsilon_{d\sigma}$, while (ii) in $Re(IV)_2F_8$$K_{d\pi}$ is slightly larger than $K_{d\sigma}$ and $\varepsilon_{d\pi}$ is much smaller than $\varepsilon_{d\sigma}$. Then, (iii) $\varepsilon_{d\pi}$ of $Re(IV)_2F_8$ is slightly larger than in $Re(IV)_2$ but (iv) $K_{d\pi}$ is clearly smaller in $Re(IV)_2F_8$. Apparently, (i) and (ii) lead to the y(dπ) > y(dσ) relation for both systems, while (iii) and (iv) lead to the fact that y(dπ) is slightly smaller in $Re(IV)_2F_8$. As seen from Figure 4, the dπ bonding and anti-bonding orbital distributions in $Re(IV)_2$ are similar to those in $Re(IV)_2F_8$, except for the ligand orbitals in $Re(IV)_2F_8$. This similarity probably originates from the smaller repulsion between the ligand and the dπ orbital than between the ligand and the dσ orbital, since the dπ orbitals do not have ring-like distributions (which are close to ligands) around each atom, contrary to the dσ orbitals. This leads to similar $\varepsilon_{d\pi}$ values for $Re(IV)_2$ and $Re(IV)_2F_8$ (see Figure 3b). However, the delocalization of dπ orbitals over the ligands in $Re(IV)_2F_8$ is found to decrease the overlap between the dπ bonding and anti-bonding orbitals of $Re(IV)_2F_8$ and thus to decrease its $K_{d\pi}$ value relative to $Re(IV)_2$ (see Figure 3b).

3.2. Equatorial ligand effect on the γ values

The bond length (R) dependences of γ for $Re(IV)_2$ and $Re(IV)_2F_8$ calculated using the UCCSD and UCCSD(T) methods are shown in Figure 5. The UCCSD(T) γ value of $Re(IV)_2$ increases, attains a maximum (γ_{max} = 2850 a.u.) at R_{max} = 2.9 Å, and then decreases. Similar γ variation is observed in $Re(IV)_2F_8$, though the γ_{max} value moves to a larger R (R_{max} = 3.6 Å) and the UCCSD(T) γ_{max} of $Re(IV)_2F_8$ (22 300 a.u.) is about 8 times as large as that of $Re(IV)_2$. Then, the UCCSD method semi-quantitatively reproduces the γ variations in the whole R region for both systems, which validates the UCCSD γ(dX) based analysis.

The major features of the γ(dσ) and γ(dπ) variations include (i) the dominant γ(dσ) contribution, in particular in the region with enhanced γ values, in contrast to the negligible dπ contributions, (ii) the bell-shape behavior of γ(dσ) with a maximum for an intermediate dσ diradical character (y(dσ) = 0.386 (at R = 2.9 Å) for $Re(IV)_2$, 0.497 (at R = 3.6 Å) for $Re(IV)_2F_8$), (iii) for small R, the larger dπ contribution for both systems, which originates from the intermediate dπ diradical characters (at R = 2.6 Å, y(dπ) = 0.619 for $Re(IV)_2$, 0.514 for $Re(IV)_2F_8$), and (iv) the similarity to the results observed in open-shell singlet bare transition-metal bonded systems [9]. As a result, the equatorial ligands have little influence on the diradical character dependences of γ in the metal–metal multiply bonded systems. On the other hand, they significantly influence the bond length dependence of γ because the ligands reduce the diradical character and thus move the R_{max} to larger R, which causes a further enhancement of γ for $Re(IV)_2F_8$ as compared to $Re(IV)_2$. The ligand effects can be interpreted as follows. As seen from the analytical formula of γ (Eq. (11) in Ref. [2]), γ is proportional to R^4/U^3, where U means the effective Coulomb repulsion in the localized NO (LNO) representation [2,35], and $U_{dX} = 2K_{dX}$. However, if considering only the variations in R_{max} and $U_{d\sigma}$, the $\gamma_{max}[Re(IV)_2F_8]/\gamma_{max}[Re(IV)_2]$ ratio amounts only to $(3.6/2.9)^4/(0.155/0.184)^3 \sim 4$, in comparison to the real enhancement ratio of *ca.* 7 (and of *ca.* 6 for γ(dσ) + γ(dπ) contributions estimated at the UCCSD level). The remaining effect can be caused by the lack of dynamical electron correlation in the UNOCASCI (2,2) U_{dX} calculations and also the other terms in Eq. (11) of Ref. [2]. In addition, the γ(dσ) of $Re(IV)_2F_8$ is negative when R < 3.0 Å, where γ(dπ) is enhanced. This seems to be related to the relatively strong third-order polarization of the dπ electrons associated with their intermediate y(dπ) values, which is accompanied by a third-order polarization of dσ electrons in the reverse direction due to the dπ–dσ electron repulsions.

4. Summary

We have investigated the diradical character dependences of the second hyperpolarizability (γ) in $Re(IV)_2$ and $Re(IV)_2F_8$ using the UCCSD and UCCSD(T) methods. Both systems show similar diradical character dependence of γ, i.e., significant enhancement of γ in the intermediate diradical character region, which is primarily caused by the dσ electron contributions. This result demonstrates that metal–metal multiply bonded complexes with equatorial ligands belong to the 'σ-dominant' third-order NLO systems like the open-shell singlet bare transition-metal bonded systems. Then, $Re(IV)_2F_8$ exhibits a smaller diradical character y(dX) ($X = \sigma$ and π) than $Re(IV)_2$ for a given metal–metal bond length, the feature of which originates from the increase of the orbital energy gap and from the decrease of the exchange integral between X-bonding/anti-bonding orbitals owing to the equatorial F ligands. Thus, the equatorial ligand effects lead to the elongation of the bond length giving intermediate y values, resulting in the

enhancement of γ_{max} by a factor of ~8 as compared to the bare $Re(IV)_2$ system. In summary, the present results confirm the validity of our y–γ correlation and predicts further enhancements of γ at a larger bond length than R_{max} for bare dinuclear systems.

Acknowledgements

This work is supported by a Grant-in-Aid for Scientific Research (No. 25248007) from Japan Society for the Promotion of Science (JSPS), a Grant-in-Aid for Scientific Research on Innovative Areas 'Stimuli-responsive Chemical Species' (No. A24109002a), MEXT, the Strategic Programs for Innovative Research (SPIRE), MEXT, and the Computational Materials Science Initiative (CMSI), Japan. It is also supported by the Academy Louvain (ARC 'Extended π-Conjugated Molecular Tinkertoys for Optoelectronics, and Spintronics') and by the Belgian Government (IUAP No P7-05 'Functional Supramolecular Systems'). Theoretical calculations are partly performed using Research Center for Computational Science, Okazaki, Japan.

Appendix A. Supplementary data

Supplementary data associated with this article can be found, in the online version, at http://dx.doi.org/10.1016/j.cplett.2013.03.030.

References

[1] M. Nakano et al., J. Phys. Chem. A 109 (2005) 885.
[2] M. Nakano et al., Phys. Rev. Lett. 99 (2007) 033001.
[3] M. Nakano et al., J. Chem. Phys. 131 (2009) 114316.
[4] M. Nakano et al., J. Chem. Phys. 133 (2010) 154302.
[5] M. Nakano et al., Chem. Phys. Lett. 418 (2006) 142.
[6] S. Ohta et al., J. Phys. Chem. A 111 (2007) 3633.
[7] H. Nagai et al., Chem. Phys. Lett. 489 (2010) 212.
[8] H. Fukui et al., J. Phys. Chem. Lett. 2 (2011) 2063.
[9] H. Fukui et al., J. Phys. Chem. A 116 (2012) 5501.
[10] K. Yoneda et al., J. Phys. Chem. C 116 (2012) 17787.
[11] K. Kamada et al., Angew. Chem. Int. Ed. 46 (2007) 3544.
[12] Z. Zeng et al., J. Am. Chem. Soc. 134 (2012) 14513.
[13] Y. Li et al., J. Am. Chem. Soc. 134 (2012) 14913.
[14] H. Kishida, K. Hibino, A. Nakamura, D. Kato, J. Abe, Thin Solid Films 519 (2010) 1028.
[15] F.A. Cotton, C.A. Murillo, R.A. Walton, Multiple Bonds between Metal Atoms, third ed., Springer, New York, 2005.
[16] M. Nishino, S. Yamanaka, Y. Yoshioka, K. Yamaguchi, J. Phys. Chem. A 101 (1997) 705.
[17] B.O. Roos, A.C. Borin, L. Gagliardi, Angew. Chem. Int. Ed. 46 (2007) 1469.
[18] S. Di Bella, Chem. Soc. Rev. 30 (2001) 355.
[19] M. Nakano et al., Theor. Chem. Acc. 130 (2011) 711.
[20] K. Yamaguchi, Chem. Phys. Lett. 33 (1975) 330.
[21] D. Herebian, K.E. Wieghardt, F.J. Neese, Am. Chem. Soc. 125 (2003) 10997.
[22] M.W. Schmidt et al., J. Comput. Chem. 14 (1993) 1347.
[23] H.D. Cohen, C.C.J. Roothaan, J. Chem. Phys. 43 (1965) S34.
[24] M. Nakano, I. Shigemoto, S. Yamada, K. Yamaguchi, J. Chem. Phys. 103 (1995) 4175.
[25] D. Andrae, U. Häussermann, M. Dolg, H. Stoll, H. Preuss, Theor. Chim. Acta 77 (1990) 123.
[26] A.W. Ehlers et al., Chem. Phys. Lett. 208 (1993) 111.
[27] G. Maroulis, D. Xenides, U. Hohm, A. Loose, J. Chem. Phys. 115 (2001) 7957.
[28] B. Champagne, E. Botek, M. Nakano, T. Nitta, K. Yamaguchi, J. Chem. Phys. 122 (2005) 114315.
[29] R. Kishi et al., J. Chem. Theory Comput. 3 (2007) 1699.
[30] T.R. Cundari, H.A. Kurtz, T. Zhou, J. Phys. Chem. A 102 (1998) 2962.
[31] T.R. Cundari, H.A. Kurtz, T. Zhou, J. Chem. Inf. Comput. Sci. 41 (2001) 38.
[32] U. Hohm, G. Maroulis, J. Chem. Phys. 121 (2004) 10411.
[33] U. Hohm, G. Maroulis, J. Chem. Phys. 124 (2006) 124312.
[34] M.J. Frisch, G.W. Trucks, H.B. Schlegel, D.J. Fox, Gaussian 09 Revision A1, GAUSSIAN Inc., Wallingford CT, 2009.
[35] C.J. Calzado et al., J. Chem. Phys. 116 (2002) 2728.